JOURNAL OF MATERIALS SCIENCE 11 (1976) 2015–2026

Spherulitic growth and recrystallization in barium silicate glasses

M. H. LEWIS, G. SMITH
Department of Physics, University of Warwick, Coventry, UK

The growth and recrystallization of spherulites formed in barium disilicate glasses between 700 and 900° C has been studied by electron microscopy and electron diffraction. Spherulites formed at 700° C consist of fibrillar (~ 100 Å diameter) monoclinic crystals in confocal arrangement with preferred crystallographic growth axes. High temperature (900° C) spherulites are composites of radially oriented plate-shaped orthorhombic crystals with lateral growth of epitaxially nucleated fibrillar monoclinic crystals. At intermediate temperatures "axialites", consisting of a single orthorhombic "midrib" crystal with monoclinic fibrillar side-growths, grow in competition with the low temperature spherulite morphology. The monoclinic fibrillar phase is believed to be an intermediate metastable structure which is able to grow more rapidly than the orthorhombic phase via cellular transformation in the presence of impurities. Brief comparison is made between the observed morphologies and theories for interface instability and cellular crystallization. Recrystallization, induced mainly by the large interfacial area of spherulite fibrils, produces faulted and twinned monoclinic grains which transform slowly to the orthorhombic stable crystal phase. A glassy intercrystalline residue becomes more prominant with grain growth.

1. Introduction

"Spherulites" are spherically shaped volumes of partially crystalline material which grow within viscous liquid matrices, under certain crystallization conditions, in organic polymers, igneous rocks and synthetic silicate glasses. Spherulite microstructures have been systematically studied in polymers. They are generally composed of radially oriented fibrillar crystals which are believed to result from crystal/liquid interface instabilities induced by impurity segregation, similar to impurity cell formation by constitutional supercooling in metallic alloy crystallization [1, 2]. This mechanism is supported by experimental observations of growth morphology with varying impurity content or crystallization temperature and comparison with simple theory for cell formation by constitutional supercooling.

In silicate glasses spherulites are frequently observed during the first stage of crystallization. They occur as an intermediate, metastable, morphology which frequently may be recrystallized to form a fine-grained, randomly oriented, polycrystalline morphology. Thus a controlled spherulitic growth and recrystallization may be a convenient process for producing silicate "glass-ceramics" with useful properties, without the need for intentional nucleation catalysis. However, the lack of a clear understanding of spherulitic growth and recrystallization mechanisms in silicates stems from the difficulty in obtaining micromorphological and crystallographic data and defining the conditions of temperature and glass composition under which spherulites grow in preference to isolated "faceted" or "dendritic" crystals.

The research described here forms part of a programme which aims to understand the mechanisms for spherulite growth and recrystallization and thereby identify the optimum conditions of spherulite structure and recrystallization treatment which result in ultrafine grained polycrystalline ceramics for structural application. In the first

phase of this work the $BaO–SiO_2$ system has been selected for study since it contains a range of glass-forming compositions in which "glass-in-glass" phase separation does not interfere with spherulite crystal growth ($3BaO \cdot 5SiO_2 - BaO \cdot 2SiO_2$, hereafter designated as $B_3S_5–BS_2$ in accepted convention). The emphasis in this initial study has been in using transmission electron microscopy and diffraction to study the micromorphological and crystallographic features of crystallization in glasses made from "laboratory grade" reagents, near to the BS_2 composition. In a future publication the effect of controlled impurity additions on crystallization of high purity glasses will be described.

2. Experimental techniques

2.1. Glass preparation and crystallization

The glasses were prepared by melting weighed mixtures of "Analar" grade $BaCO_3$ and "pure precipitated" SiO_2 (supplied by Hopkin & Williams Ltd) in platinum crucibles. The glasses were homogenized by crushing and remelting, then finally rapidly cooled in thin plate form by pressing between graphite-coated steel plates.

The thin (1 to 2 mm) glass plates were isothermally crystallized for varying times between 650 and 900° C in the atmosphere.

2.2. Microscopy

Thin sections for transmission–optical microscopy were prepared by gluing the heat-treated, 1 to 2 mm plates to a glass microscope slide with Araldite resin and lapping to a thickness of 30 to 50 μm. Thin sections for electron microscopy were prepared from the bulk glass by ion-beam sputtering after mechanical thinning. The plates were first ground to a thickness of < 1 mm, then cut into 3 mm diameter discs with an ultrasonic treppaning tool. The disc centres were profiled to near perforation with a rotating diamond tool. The profiled discs were placed in an ion-beam machining apparatus and sputtered to perforation using 5 kV argon ion beams incident on both surfaces at an angle of 40°. Both surfaces of the perforated disc were given a thin carbon coating (by rapid vacuum evaporation) to eliminate charging in the electron microscope. Use of a 200 kV electron microscope was found to be an important advantage (over 100 kV) in reducing the susceptibility of specimens to irradiation damage, especially in the glassy state. However, the large angle double-tilt stage fitted to the 100 kV instrument was essential for determining reciprocal lattices for silicate phase identification.

3. Spherulite growth and recrystallization

3.1. Optical micrography

A cursory optical examination to establish convenient heat-treatment times and temperatures is exemplified in Fig. 1 and a summary of the progress of transformation for different temperatures

TABLE I

Temperature (° C)	Time					
	5 min	1 h	5 h	20 h	150 h	1000 h
700	–	Spherulites in glass matrix	Spherulites in glass matrix (Fig. 1a)	Impingement of spherulites	Completely spherulitic	Recrystallized (mainly monoclinic)
750	–	Spherulites and few axialites in glass matrix	Impingement of spherulites and start of recrystallisation	Recrystallized		
800	–	Spherulites and axialites in glass matrix	Spherulites and axialites, impingement complete and start of recrystallization	Recrystallized (mixed orthorhombic and monoclinic)		Recrystallized (mainly orthorhombic) (Fig. 1c)
900	Large spherulites start of recrystallization (Fig. 1b)	Recrystallized				

is presented in Table I (for BS_2 composition). Reference is made later in the text to the orthorhombic and monoclinic crystal symmetries mentioned in this table.

Subsequent crystallization treatments were restricted to the temperature interval 700 to 900° C since below 700° C spherulites form extremely slowly and above 900° C spherulites grow and recrystallize uncontrollably within a few minutes. Between these temperatures there is a marked change in spherulite nucleation and growth rates, e.g. in Fig. 1a and b spherulite diameters are

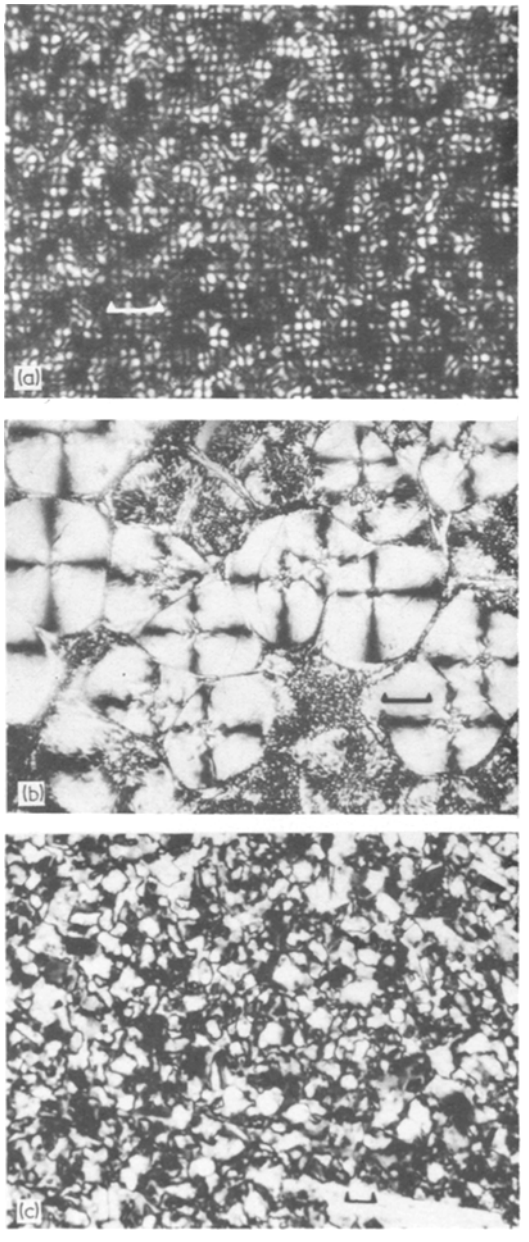

Figure 1 Polarized light optical micrographs showing spherulites after (a) 5 h at 700° C, (b) 5 min at 900° C. (c) Recrystallized structure after 1000 h at 800° C. Magnification markers in (a) (b) and (c) are 10, 100 and 100 μm respectively.

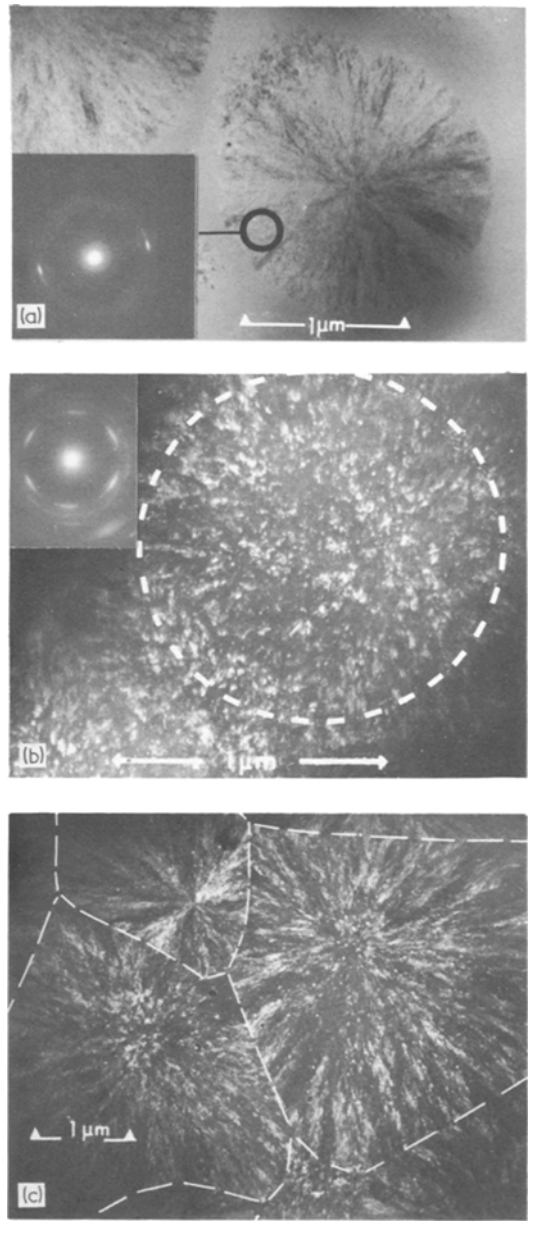

Figure 2 Electron microscope images of low temperature fibrillar spherulites; (a) diametrical section in bright field with preferred fibril axis indicated by inset diffraction pattern; (b) transverse section, in dark field, through a group of fibrils from a single spherulite; the preferred rotational orientation about fibril axes is demonstrated by the inset diffraction pattern; (c) dark-field image of a group of spherulites following impingement after 170 h at 700° C.

~3 and 300 μm corresponding to heat-treatment times of 5 h and 5 min respectively. Most of the size increase occurs between 800 and 900° C and in the following sections will be shown to be mainly the result of a change in the spherulite micromorphology and crystallography.

3.2. Spherulite growth morphology

An electron microscope study of the disilicate (BS_2) glass crystallized at 700° C for up to 170 h reveals the progressive growth and impingement of spherulites composed of extremely fine (~100 Å diameter) fibrillar crystals in radial orientation. The volume of crystalline material is surprisingly small, neighbouring fibrils being separated by ~1000 Å in a glass matrix (Fig. 2a to c). This feature produces weak diffraction contrast in electron microscope images (Fig. 2a) and the fibrillar structure is best imaged in dark field (Fig. 2b and c). In Fig. 2a and b the spherulites are isolated in a glass matrix and retain their overall spherical shape, resulting from uniform radial fibrillar growth. In specimens crystallized for longer times the spherulite identity is lost by mutual impingement (Fig. 2c), but there is little change in the fibril diameter and hence in crystalline volume fraction up to the onset of recrystallization.

Electron diffraction confirms the radially preferred crystallographic growth axis for the fibrils (resulting in the characteristic "orthogonal-cross" contrast when complete spherulites are imaged with transmitted polarized light Fig. 1a). Electron diffraction patterns from spherulites contain three prominent closely spaced rings which have a spread in radii encompassing the diffuse ring of weak electron scattering from the parent glass. The patterns inset in Fig. 2a and b are recorded from small selected areas of spherulite in which the fibrils are in longitudinal and tranverse section respectively. Hence the preferred growth axis is approximately parallel to a reciprocal lattice vector identified by the middle diffraction ring (Fig. 2a). The diffraction pattern from a transverse-fibrillar section (Fig. 2b) shows that neighbouring fibrils are not randomly oriented with respect to rotation about the preferred growth axis. Thus it is likely that a large group of neighbouring fibrils evolve by a branching process from a common origin, to maintain uniformity of interfibrillar spacing during radial growth. The arcing of the diffraction spots (on the inner ring position) with pseudo-hexagonal symmetry (Fig. 2b) indicates a spread of ~10° in rotation about the growth axis which may be caused either by elastic twisting of fibrils or introduction of low angle boundaries during a fibril branching process. The analysis of "axialites" which grow in competition with spherulites at higher temperatures indicates that the latter explanation is more probable.

"Axialites" are so-called because of the loss of overall spherical symmetry of the fibrillar structure. They are visible as a minor feature of the microstructure following 750° C heat-treatment but form the dominant crystal morphology at 800° C. They consist of a comparatively large central "midrib" crystal from which lateral growth of fibrils occurs with the same dimensions and preferred growth axis observed in spherulites (Fig. 3a to d). Thus growth of "axialites" in preference to spherulites occurs whenever there is prior nucleation of morphologically asymmetrical crystals such that their elongated faces act as heterogeneous nucleants for the fibrillar morphology. The crystallographic description given below shows that the midrib and fibrillar structures are separate silicate phases and that the fibrillar phase is epitaxially nucleated on the surfaces of the midrib plate-like crystal.

The apparent reversion to a spherulite morphology with a large increase in growth rate at higher temperatures (Fig. 1c) is also explicable via a two-phase structure. Thus images from small sections of these large spherulites have an axialitic structure (Fig. 4). The "midrib" phase is, in this case, growing with a spherulitic morphology consisting of branching elongated platelets crystals. However, the spacing between the radially oriented branching crystals is occupied by lateral growth of the fibrillar phase which has epitaxially nucleated on the spherulite plates (Fig. 4). The branching process maintains a small spacing between "midrib" plates ($< 1\,\mu m$) and restricts the fibrillar growth via impingement at smaller distances than in "axialites" (in which the midrib phase spacing is usually $> 1\,\mu m$).

3.3. Crystallography

The crystallographic identity of "midrib" and fibrillar phases is similar in spherulites, axialites and "composite" spherulites which grow at high temperatures. In view of the absence of crystal structure analysis, conflicting powder-diffraction data and similarity in d spacings for the many reported phases in the $BaO–SiO_2$ systems, reci-

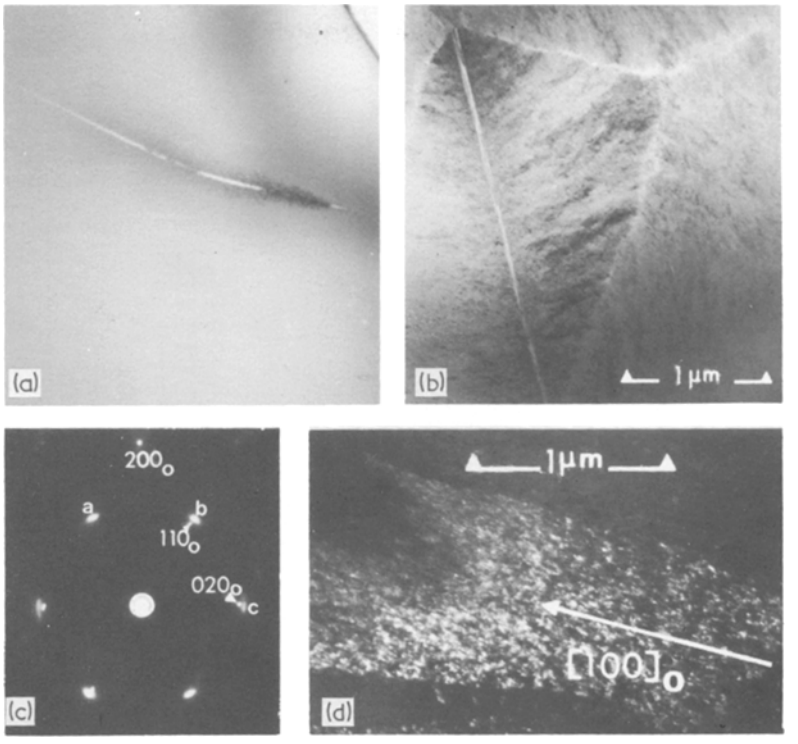

Figure 3 "Axialites" composed of orthorhombic "midrib" phase and epitaxially nucleated monoclinic fibrils: (a) the growth edge of an orthorhombic plate with small fibrillar projections; (b) after impingement; (c) diffraction pattern showing epitaxy of monoclinic fibrils (reflections a, b, c) on orthorhombic (o) plate with, (d) corresponding selected-area dark-field imaged with reflection a.

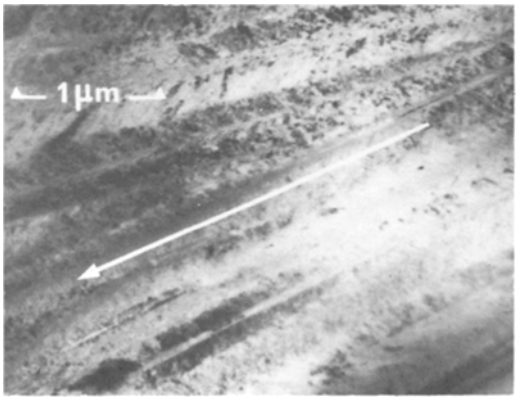

Figure 4 Bright-field image of part of a large "composite" spherulite consisting of branching orthorhombic crystals and fibrillar (monoclinic) side-growths. The radial growth axis of the spherulite is indicated by the arrow.

procal lattices have been constructed from electron diffraction patterns from recrystallized grains in BS_2 specimens. Thus an interpretation of the diffraction patterns from spherulites and axialites is possible using the reciprocal lattices from two different recrystallizing phases. Fig. 5 is an example

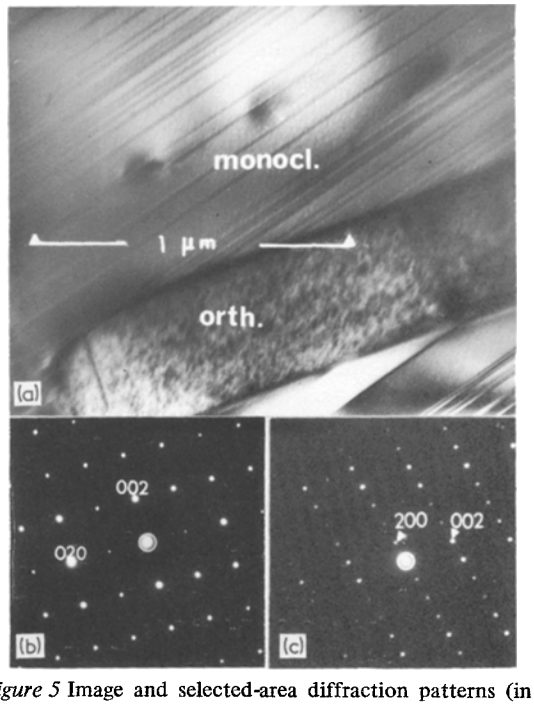

Figure 5 Image and selected-area diffraction patterns (in correct relative orientation) from orthorhombic (b) and monoclinic (c) disilicate phases formed on recrystallization.

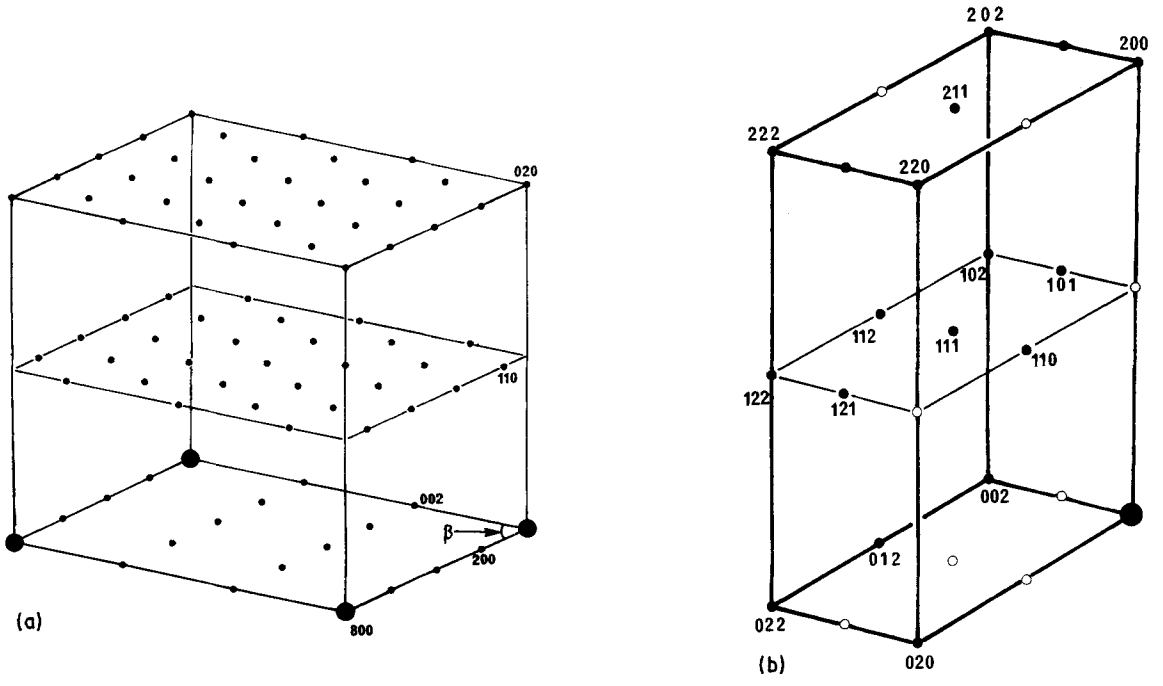

Figure 6 Reciprocal lattices for (a) monoclinic and (b) orthorhombic symmetry structures, constructed from single grain diffraction patterns on the type shown in Fig. 5.

of diffraction patterns from a recrystallized area of BS_2 containing the two phases and Figs. 6a and b are sketches of the reciprocal lattices of their monoclinic and orthorhombic symmetry structures. The orthorhombic phase is identified as the naturally occurring disilicate "sanbornite" which has a structure of $n(Si_4O_{10})^{4-}$ layers parallel to (0 0 1) bonded with Ba^{2+} ions lying midway between layers [3]. The "midrib" phase in axialites and composite spherulites has been identified as the sanbornite structure from single crystal diffraction patterns such as Fig. 3c in which orthorhombic reflections are indexed. This pattern corresponds to the selected-area dark-field imaged in Fig. 3d, with the electron beam normal to the plate-shaped crystal (parallel to $[0\,0\,1]_0$). Hence the preferred plate-growth directions are parallel to the $n(Si_4O_{10})^{4-}$ layers and the maximum plate dimension is normally $[1\,0\,0]_0$.

The fibrillar phase is more difficult to identify since it is present in small volume fraction in a glassy matrix and has a spread in orientation within groups of fibrils. This results in relatively weak and diffuse diffraction compared with the sharp spot patterns from the orthorhombic "midrib" single crystals. However, the patterns are sharper for "axialites" due to the small spread in rotational orientation about the fibril axis due to epitaxial nucleation and the absence of profuse branching, resulting from parallel growth from multiple nucleation sites.

A prominent pattern from both spherulite and axialite fibrils is inset in Fig. 7b. This figure gives an interpretation of the observed diffraction pattern and dark-field image (Fig. 7a) recorded with the electron beam approximately normal to the fibril axis (or parallel to the "midrib" crystal face. In Fig. 7c the single crystal pattern from the monoclinic-symmetry phase (see e.g. Fig. 5 or the reciprocal lattice in Fig. 6a) is superposed on the arced ring-pattern. The correlation is satisfactory if the very weak diffuse reflections 0 0 2 and 2 0 2 are included (these are only visible on original diffraction pattern negatives and are always in the approximate direction of the fibril axis). The fibril axis is parallel to the 1 0 2 reciprocal lattice vector, the 2 0 4 reflection forming part of the prominant middle ring in all patterns. The other strong reflections coincide with the prominent inner ring and may be indexed as $\bar{8}\,0\,2$ (monoclinic) corresponding to one of the strongest reflections from the densely populated reciprocal lattice plane in Fig. 6a. Reflections labelled 1 and 2 in Fig. 7b (inset) do not always occur

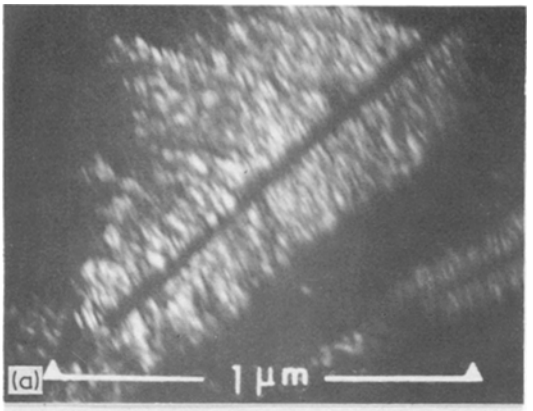

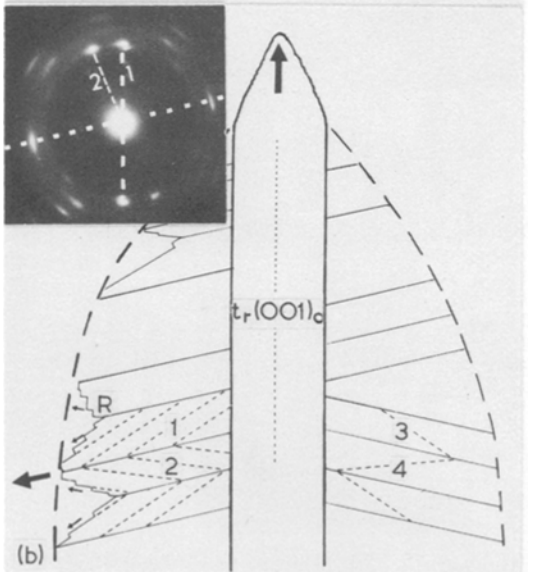

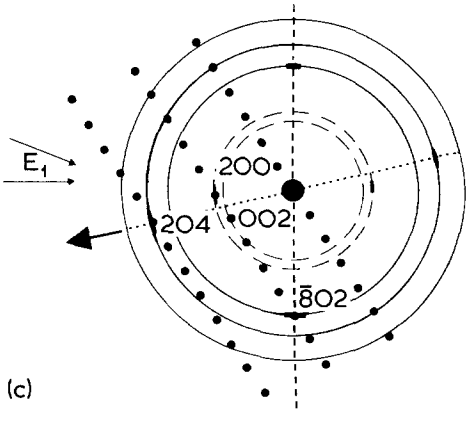

Figure 7(a) Dark-field image of "axialite" fibrils in longitudinal section. (b) and (c) Interpretation of the crystallography of axialites and composite spherulites with inset diffraction pattern and monoclinic reciprocal lattice plane (c) in correct relative orientation. The dotted lines labelled 1, 2, 3 and 4 are traces of possible (1 0 0) monoclinic twin or fault planes found in recrystallized grains.

together, particularly from very small selected areas, but can be interpreted as originating from twin-related sets of fibril crystals in the manner depicted in Fig. 7b.

The diffraction pattern in Fig. 3c is a sharper version of that inset in Fig. 2b and is characteristic of that from fibrils nearly parallel to the electron beam. Fig. 3d is a dark-field image using a "fibril reflection" (labelled a in Fig. 3c). The epitaxial orientation relation, referred to above, is demonstrated in Fig. 3c with an obvious correspondence between reflections b and c with the 1 1 0 and 0 2 0 orthorhombic reflections, respectively. This pattern may be explained on the basis of a combination of two reciprocal lattice planes for the monoclinic phase. Thus reflections c and b are monoclinic reciprocal lattice points $\bar{8}02$ and $\bar{3}12$ lying on reciporcal lattice planes (normal to Fig. 7c) which enclose an angle of $\sim 30°$ and would normally appear in diffraction patterns for the two electron beam directions labelled E_1 in Fig. 7c. Reflections b and c normally appear in the same pattern (with the 0 2 0 monoclinic reflection) because of the variations in fibril axis due to elastic bending and, in the spherulite case, low-angle branching. The variation in dark-field contrast along the fibrils (e.g. Fig. 7a) is further evidence for elastic bending during lateral growth from the midrib phase.

3.4. Recrystallization

Following the impingement of spherulites, axialites and "composite" spherulites the microstructure is transformed to a polycrystalline ceramic via recrystallization. Approximate times at which recrystallization is first observed varies from 5 min at 900° C to > 170 h at 700° C (Table I) for the disilicate composition. Microstructural and diffraction evidence indicates that the recrystallization produces two distinct phases with monoclinic and orthorhombic reciprocal lattices which have been constructed from single-grain electron diffraction patterns, as previously described (Fig. 6). The first formed phase in the fully spherulitic structure at 700° C has monoclinic symmetry (lattice parameters $a = 32.95$ Å, $b = 4.69$ Å, $c = 13.98$ Å, $\beta = 82°$). This is progressively transformed to the orthorhombic form ("sanbornite" with lattice parameters $a = 4.68$ Å, $b = 7.64$ Å, $c = 13.58$ Å) after long annealing. This is also true at the higher temperatures except that the proportion of orthorhombic phase present in the early stages of

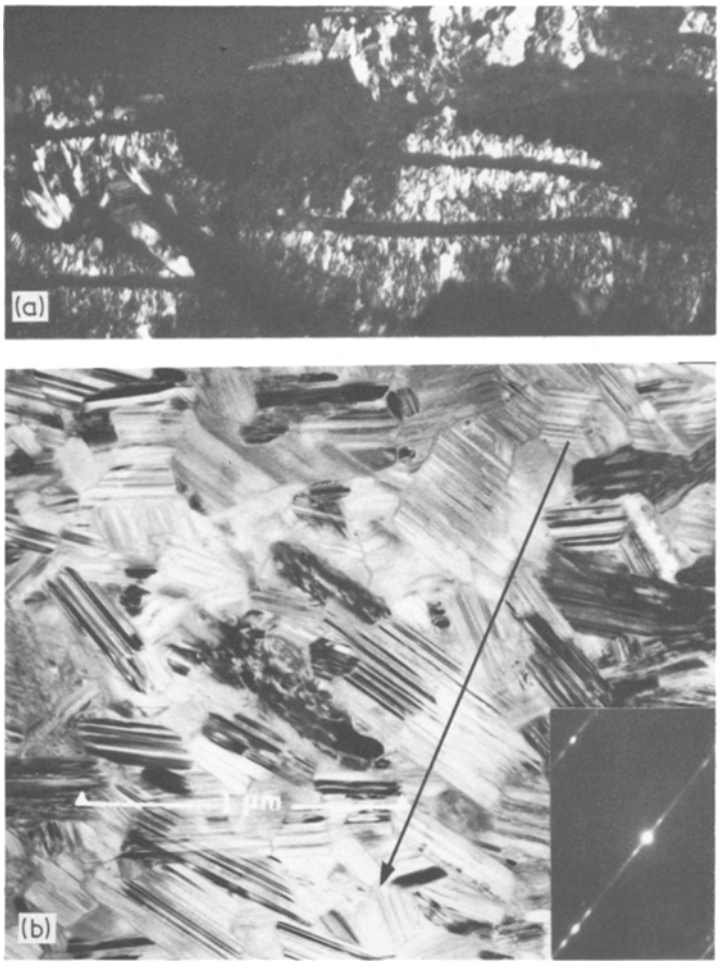

Figure 8(a) Initiation of recrystallization within axialite fibrils, shown in dark field. (b) Small, highly faulted and twinned, monoclinic crystals in a recrystallized composite spherulite. Single grain diffraction patterns contain extended reciprocal lattice points (inset) due to the high fault density. The radial growth axis for the composite spherulite, which results in a preferred recrystallization texture over small volumes, is indicated by the arrow.

recrystallization is greater, since it is already present as part of the axialites and composite spherulites.

The "recrystallization" is observed as a competitive growth of fibril crystals following a very slow thickening in the glass matrix (Fig. 8a). Hence the preferred orientation within groups of fibrils is conserved and is particularly prominent in axialites due to the epitaxial fibrillar growth on a single orthorhombic midrib crystal. Recrystallizing monoclinic grains contain a large density of stacking faults and lamellar micro-twins (Fig. 8b) which result in an elongation of diffraction spots normal to the (1 0 0) fault and twin plane (Fig. 8b inset). Thus fibril orientations 1 and 2 (in Fig. 7b) and their symmetrically equivalent orientations 3 and 4 give rise to four twin/fault plane orientations (see dotted lines in Fig. 7b) which may be identified in Fig. 8b. This image is recorded from the first stages of recrystallization in a "composite" spherulite (at 900° C) in which neighbouring midrib plates have similar orientation (indicated by the arrow). Any preferred orientation is lost as grain growth produces ~ 1 μm size crystals, i.e. in excess of the size of the nucleating fibrillar groups within which preferred orientation exists. In addition much of the lamellar micro-twinning and faulting is removed by longer annealing, producing microstructures such as Fig. 9. The recrystallized morphology is different for orthorhombic and monoclinic grains and reflects the anisotropy of crystal growth. Orthorhombic grains are generally thick plates with maximum growth rate parallel to the fault or silicate layer

plane, as observed in axialites. Monoclinic grains are more equi-axed but frequently exhibit faceted surfaces parallel to (1 0 0) and (0 1 0) and (0 0 1). It is clear that faceted grains in random orientation cannot completely fill space and the presence of an intercrystalline glassy residue can be detected by the absence of diffraction contrast (Fig. 10). The glass phase becomes more prominent with progress of grain growth because of the decrease in grain-boundary area in unit volume of polycrystal.

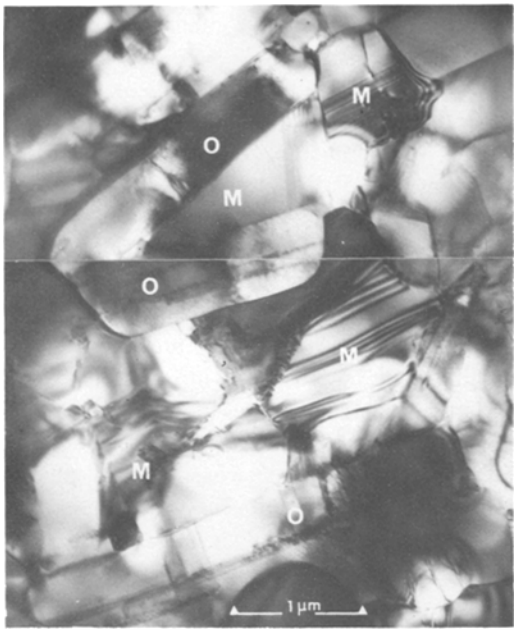

Figure 9 Mixed orthorhombic (o) and monoclinic (m) symmetry crystals following grain growth and partial transformation (after 20 h at 800° C).

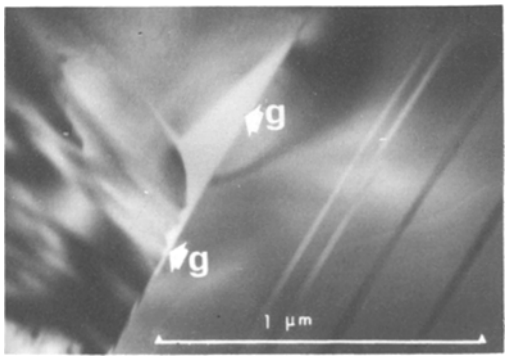

Figure 10 Large faceted monoclinic crystals enclosing residual glass phase (g) after extensive grain growth (1000 h at 700° C).

4. Discussion

4.1. Spherulite growth mechanisms

A distinction has been made between low-temperature spherulites and the comparatively large high-temperature "composite" spherulites in terms of the first crystallizing phases. The high-temperature spherulite morphology is dominated by the rapid edgewise platelet growth and profuse branching of the orthorhombic disilicate phase. The resulting structure is relatively coarse with inter-platelet spaces filled by lateral growth of the monoclinic disilicate phase which occurs in the fine-fibrillar morphology found in low-temperature spherulites. At intermediate and high-temperatures it is present only following heterogeneous (epitaxial) nucleation on orthorhombic plate surfaces. "Axialites" are distinguished from the high-temperature spherulites because growth and branching of single orthorhombic plates is inhibited by the more rapid growth of the monoclinic fibrillar phase. While differences in growth morphology of high and low temperature "spherulites" may be ascribed to differences in crystallization kinetics and growth anisotropy of the different crystallizing phases, the reasons for fibrillation and repetitive branching, necessary for spherulite formation, are not clear.

Under conditions of slow crystal growth in a high-viscosity pure silicate melt, the expected morphology is that of isolated faceted crystals, bounded by low-index planes, with a shape dictated mainly by anisotropy in growth kinetics. This morphology is observed for recrystallized grains and during the initial stages of growth of the orthorhombic phase (e.g. Fig. 3). A single crystal dendritic morphology is not observed because, (i) the rate of growth, (and therefore of latent heat generation), is small and, (ii) it would require cellular growth of the strongly faceting (0 0 1) orthorhombic interface, parallel to the (Si_4O_{10}) layer structure. An alternative is the formation of twin crystal branches from the primary plate, thus overcoming the lateral growth problem by provision of re-entrant edge nucleation sites [4]. This process is suppressed in favour of epitaxial nucleation of the monoclinic fibrillar phase and at a later stage by "defoliation" of the advancing platelet parallel to the silicate layer plane and elastic bending of the separating crystals.

The monoclinic phase nucleates and grows preferentially at lower crystallization temperatures. It is suggested that this preference stems from the

ability of this crystal structure to grow more rapidly with a cellular (fibrillar) morphology in the presence of segregated impurities. Thus the presence of an impurity layer at the growth interface will suppress further crystallization if the impurity inhibits mobility of the crystallizing species. The problem is partly overcome by modifying the interface shape to form fibrillar projections which reject impurities laterally into the inter-fibrill spaces. This alternative crystallization morphology is applicable only to non-faceting or weakly-faceting crystal interfaces, hence may be applicable only to the monoclinic structure. The mechanism for initiation of the fibrillar interface follows the suggestion of Keith and Padden [1] of a constitutional supercooling effect produced by the impurity "layer" at the interface of slow growing polymer crystals under nearly isothermal conditions. Evidence in favour of this model for spherulitie growth has been given from observed variations in fibril size and spacing with impurity content or growth temperature and a comparison with "theoretical" predictions of variation in "wavelength" for the instability at the initially planar interface. This is related to δ, the "thickness" of an impurity layer which, in turn, is determined by the ratio D/G, where D is the impurity diffusion coefficient and G the crystal growth rate. Hence, when the impurity diffusion is slow and crystal growth is rapid, δ is small and fine fibrils are predicted. The variation of crystal growth rate with temperature ($\mathrm{d}G/\mathrm{d}T$) may be either positive or negative (for large or small ΔT respectively) while $\mathrm{d}D/\mathrm{d}T$ is always positive. Hence the greatest variation in δ (and therefore in fibril size) is expected for small ΔT. This condition is not applicable to BS_2 crystallization in which spherulites grow 600 to 800° C below the equilibrium melting temperature, where $\mathrm{d}G/\mathrm{d}T$ is observed to be positive. Analysis of higher-temperature spherulites of the monoclinic phase is inhibited by the appearance of the orthorhombic form which grows in much coarser morphology. Even when the monoclinic phase appears as a secondary product of high-temperature crystallization its fine fibrillar morphology is unchanged; this may result from a balance of the variation of D and G with temperature of from a limiting size dictated by capillarity [5].

The origin of the "impurity" layer causing interface instability in BS_2 crystals is uncertain. The identity of the monoclinic recrystallized phase and fibrillar spherulitic phase has been tentatively established and this is supported by recent observations of a correlation between a different monoclinic phase in recrystallized B_3S_5 compositions and its fibrillar spherulitic precursor. Hence there is no evidence for a marked composition difference between parent BS_2 glass and spherulite crystals which would promote diffusion-controlled initial growth and subsequent interface instability. Small accidental deviations from stoichiometric BS_2 composition are not believed to be important because of the insensitivity of crystal morphology to intentional deviations between composition limits 35% BaO to 28% BaO (towards the SiO_2-rich limit, axialites occur at lower temperatures but are morphologically similar). It is probable, therefore, that accidental impurities in the "Analar" starting materials are responsible for fibrillation.

One of the difficulties in application of the "interface instability" mechanism to explain the fibrillar morphology is the absence of microscopic evidence for cellular breakdown of an initially planar interface. Thin film diametrical sections through spherulites (e.g. Fig. 2) show that fibrillation occurs immediately on nucleation. Etched surfaces show heterogeneities at spherulite centres, suggesting heterogeneous nucleation or a discontinuity in morphology, but this is clearly a differential etching effect. These observations, together with a branching of fibrils (during radial growth) to maintain a constant fibril spacing suggest that spherulite growth may alternatively be interpreted as a form of cellular (discontinuous) precipitation. The cellular transformation in impure barium silicate glasses may be represented:

(BS_2 parent glass + impurity) → BS_2 (pure crystal) + (BS_2 product glass + segregated impurity).

The composition change is achieved by lateral diffusion of impurity from the tips of growing fibrils, resulting in linear growth kinetics for the cellular product. The mean fibril thickness will be controlled both by the inter-fibril spacing and concentration of impurities between them, which reduces the effective supercooling for crystallization and for certain impurities, increases the viscosity of the glass. The interfibril spacing (δ) is again expected to vary with spherulite growth rate G and impurity diffusivity D as $\delta = \text{constant}\ (D/G)$. In this case δ, is inversely proportional to

G because the lateral diffusion distance is related to δ. The value of δ will be determined by a balance between minimization of diffusion distance and interfacial energy in unit volume between crystal and impurity enriched glass. Hence a small value for specific interfacial energy between glass and crystal should result in a fine fibril formation. The variation of δ with crystallization temperature is predicted to be similar to that for the "interface instability" model.

Current research in this laboratory [6] using high purity materials shows that specific added impurities have a pronounced influence on crystallization morphology in barium silicate glasses. The results of this work should enable a more precise prediction of crystallization mechanism with varying crystal type, impurity distribution coefficient and its effect on interface viscosity, and a possible quantitative correlation with a cellular crystallization model.

4.2. Recrystallization

The disilicate glass recrystallizes at all temperatures to form a mainly monoclinic polycrystalline microstructure. The occurrence of more of the orthorhombic phase on initial recrystallization at higher temperatures can be traced to its prior growth as components of axialites and composite spherulites. Because the recrystallized microstructures are slowly transformed to the orthorhombic "sanbornite" form at all temperatures it is believed that the monoclinic phase is a kinetically preferred metastable disilicate in both spherulite growth and recrystallization. The orthorhombic structure has previously been referred to as the "low-temperature" polymorph of BS_2 although in glass crystallization studies [7] this has not been positively identified as the sanbornite structure. A phase of lower but unidentified symmetry, formed from the glassy state and by direct reaction of BaO and SiO_2, has been referred to as the "high temperature" polymorph [8]. However, Douglass [3], who has determined the "sanbornite" structure, has found no other phase when the mineral is heated near to its melting point or when $BaO + 2SiO_2$ powders are sintered at 1375 to 1450° C. A comparison of published X-ray powder diffraction data from the "high temperature" polymorph [8] shows that most reflections can be identified with the reciprocal lattice of the proposed monoclinic metastable form. However, some of the anomalies in lattice spacings and the occurrence of extra reflections in powder patterns can be explained in terms of a mixture of orthorhombic and monoclinic phases.

In demonstrating that fibrillar and first recrystallized monoclinic phases are similar, it may be concluded that the main driving-force for the recrystallization is the reduction in the large interfacial energy per unit volume of the fibrillar phase. The fine fibrillar morphology provides a very large nucleation density for recrystallized grains, in the absence of intentional nucleation catalysts. An important feature of microstructures recrystallized from axialites or composite spherulites is the presence of anomalously large plate-shaped orthorhombic crystals (Fig. 1c). These are believed to originate from a coarsening of the orthorhombic platelets already present before recrystallization and are expected to be detrimental to mechanical behaviour in providing regions of stress concentrations for crack nucleation. Hence the preferred path to formation of a silicate ceramic with fine and uniform grain size is to form a completely fibrillar spherulitic structure at low temperatures followed by a higher temperature recrystallization.

During recrystallization an additional component of free-energy change for the transformation stems from a removal of the large volume fraction of glassy phase remaining after spherulite growth. However, it has been shown by direct observation that for a moderately pure glass of stoichiometric BS_2 composition, crystallization is incomplete. The main factors which prevent the complete removal of intercrystalline glass residues are: (i) a reduction in the effective undercooling or diffusion rate required for crystallization by segregation of impurities to the glass phase, and (ii) the very slow normal growth of "faceted" crystal faces which form the most prominant enclosure for glass residues. Even for laboratory reagent materials the concentration of segregated impurities in the small volume of residual glass can be large. Experiments are in progress using ultra-high purity glasses in an attempt to assess the relative importance of impurity and crystallographic factors in preventing complete crystallization.

The presence of a grain-boundary glassy phase and its viscosity is an important factor controlling high-temperature deformation and delayed fracture. Its presence may be beneficial in inhibiting grain growth, since boundary migration must involve a dissolution–reprecipitation process. It is not clear that this process is kinetically unfavour-

able in relation to diffusional transfer of atoms across a "pure" solid-state grain boundary especially if the boundary phase has a low viscosity. During a typical grain-grwoth process at 800° C, grain sizes increase from $\sim 1\,\mu$m (after a 20 h heat-treatment) to $\sim 100\,\mu$m (after 1000 h) and this is accompanied by an increase in the proportion of orthorhombic phase. It is probable that both grain-growth inhibition and high-temperature properties could be improved using ceramics prepared from high-purity glasses or glasses with selected impurity additions which either increase residual phase viscosity or form segregates of atomic dimensions which reduce grain-boundary energies and hence inhibit boundary migration. One of the problems in general application of these principles to other ceramics formed by spherulite recrystallization lies in removing a relatively low viscosity residual glass phase which may, via viscous flow, accommodate changes in atomic volume on recrystallization, thus preventing internal crack nucleation.

Acknowledgements

The receipt of continuing financial support for this work from the Science Research Council, is gratefully acknowledged.

References

1. H. D. KEITH and F. J. PADDEN, *J. Appl. Phys.* **34** (1963) 2409.
2. *Idem, ibid* **35** (1964) 1270.
3. R. M. DOUGLASS, *Amer. Mineral.* **43** (1958) 512.
4. R. S. WAGNER, *Acta Met.* 8 (1960) 57.
5. J. W. CAHN, "Crystal growth", edited by H. S. Peiser (Pergamon, Oxford, 1967) p. 681.
6. J. METCALF-JOHANSEN, unpublished work, University of Warwick, 1976.
7. D. G. BURNETT and R. W. DOUGLAS, *Phys. Chem. Glasses* **12** (1971) 117.
8. S. R. ROTH and E. M. LEVIN, *J. Res. Nat. Bur. Stand.* **62** (1959) 193.

Received 9 March and accepted 2 April 1976.